Journal of Molecular Catalysis B: Enzymatic 70 (2011) 88–94

Contents lists available at ScienceDirect

Journal of Molecular Catalysis B: Enzymatic

journal homepage: www.elsevier.com/locate/molcatb

Identification of novel esterases for the synthesis of sterically demanding chiral alcohols by sequence-structure guided genome mining

Giang-Son Nguyen[a,1], Mark L. Thompson[a,b,1], Gideon Grogan[b], Uwe T. Bornscheuer[a], Robert Kourist[a,c,*]

[a] Institute of Biochemistry, Department of Biotechnology & Enzyme Catalysis, University of Greifswald, Felix-Hausdorff Str. 4, 17487 Greifswald, Germany
[b] York Structural Biology Laboratory, Department of Chemistry, University of York, YO10 5DD, York, United Kingdom
[c] Chair of Chemistry of Biogenic Resources, TU München, Schulgasse 16, D-94315 Straubing, Germany

ARTICLE INFO

Article history:
Received 15 November 2010
Received in revised form 11 February 2011
Accepted 14 February 2011
Available online 21 February 2011

Keywords:
Esterase
Enantioselective
Tertiary alcohol
Functional screening
Genome mining

ABSTRACT

Six esterases isolated from sequence and structure-guided genome mining approaches were evaluated for the kinetic resolution of secondary and tertiary alcohols that find application in the fine chemical and pharmaceutical industries. Activity and enantioselectivity with *E*-values of up to 24 were determined towards a range of sterically demanding tertiary alcohol esters. Excellent enantioselectivity ($E > 100$) was also achieved in the hydrolysis of a less challenging secondary alcohol ester, menthyl acetate. These results highlight that these approaches can be used for the identification of novel esterases applicable to the preparation of commercially desirable alcohols.

1. Introduction

Tertiary alcohols (TAs) have become interesting targets for organic synthesis either in their own right, as flavour fragrance compounds, or as building blocks for valuable pharmaceutical compounds [1,2]. In the first instance, linalool is widely used in fragrance products such as perfumes, soaps and detergents, whilst also being important as an odour-active component in the hopping of beer [3]. Gossonorol, originally isolated from the cotton plant (*Gossypium*), possesses a floral scent, and is often contained within oils extracted from medicinal plants [4]. It has also attracted interest as a precursor in the synthesis of other compounds used in biologically active remedies [5,6]. In terms of pharmaceutical precursors, tertiary cyanohydrins are versatile precursors for the syntheses of α-hydroxy acids, β-amino alcohols and β-hydroxy amides [5]. Pyridine-derived tertiary alcohols have been used as building blocks for the synthesis of A_{2A} receptor antagonists, promising compounds for the therapy of Parkinson's disease [6]. Ekegren et al. [7] have also described a new class of HIV-1 protease inhibitors containing a tertiary alcohol in the transition-state mimicking scaffold. In the search for a therapy for Alzheimer's disease, a new class of compounds based on BACE-1 inhibitors containing the tertiary alcohol motif has also been investigated [8].

Biocatalytic routes employing enantioselective hydrolases offer promise in the preparation of enantiopure TAs, but have thus far failed to achieve their potential owing to the sterically demanding nature of these substrates. For example, there have been reports of the application of both whole-cell preparations of bacteria or cell-extracts to the production of enantio-enriched linalool by hydrolysis of racemic linalyl acetate [9–11]. Whole cells of *Rhodococcus ruber* DSM 43338 hydrolysed linalyl acetate to give (*S*)-linalool with a conversion of 25%, an enantiomeric excess (*ee*) of 56%, and a selectivity (*E*) of 4.2 [9]. An isolated enzyme EstA from *Rhodococcus* sp. was applied for the enantioselective hydrolysis of linalyl acetate [12], however the enantioselectivity was again modest ($ee_P = 45\%$ at 20% conversion, and $E = 3$) and suggests there may be considerable scope for improvement. In targeting therapeutically valuable pyridine-derived TAs, a recent study showed that some recombinant esterases have excellent enantioselectivity against the nitrogen-bearing TA esters [13], however the substrate range of the individual enzymes was quite limited. Recently [13] we developed a straightforward chemoenzymatic route to the chiral tertiary alcohol (*S*)-2-hydroxy-2-methylbutyric acid, which occurs naturally in clerodendrin-A [14], and has also been used as a precursor for the synthesis of a cyclooxygenase inhibitor [15]. Two

* Corresponding author at: Group of Biochemistry and Enzymology, Chair of Chemistry of Biogenic Resources, TU München, Schulgasse 16, D-94315 Straubing, Germany. Tel.: +49 3834 8622817; fax: +49 9421 187 310.
E-mail address: kourist@tum.de (R. Kourist).
[1] These authors contributed equally to this work.

1381-1177/$ – see front matter © 2011 Elsevier B.V. All rights reserved.
doi:10.1016/j.molcatb.2011.02.009

enzymes, each displaying moderate enantioselectivity, were identified from that study; a thermostable esterase A from *Pyrubaculus calidifontis* and the metagenome-derived esterase Est8. Interestingly, both belong to the family of hormone-sensitive-lipase-like enzymes and share a high sequence similarity.

In this paper, we report the further investigation of hydrolytic enzymes for the hydrolysis of TAs, using two complementary approaches. First, the genome sequence of the actinomycete *N. farcinica* IFM10152 [16], was screened for the presence of esterase genes encoding enzymes containing the GGG(A)X motif, which is known to confer activity of these enzymes towards TAEs [16]. The cloning, expression and characterisation of activity and enantioselectivity, with particular focus on chiral tertiary alcohols, for two of these esterases (EstA1 and EstA2), is described herein.

Second, we used the new α/β-Hydrolase Fold Enzyme Family 3DM Database (ABHDB), which is a structure-based classification of 12,431 available sequences of α/β-hydrolase fold enzymes, to search for enzymes with high similarity to esterase A from *P. calidifontis* and the metagenome-derived esterase Est8, and which may therefore show potential for improved enantioselectivity in the kinetic resolution of TAEs. The ABHDB facilitates a deeper analysis of structure–function relationships within this diverse class of enzymes [17] and was recently applied as a tool for the prediction of key residues for the engineering of the enantioselectivity of an esterase [18] and for the guidance in library generation for protein engineering [19,20]. These complementary approaches have proved to be successful in unearthing new esterase activities towards sterically demanding TA esters of relevance to both flavour/fragrance and pharmaceutical chemistry.

2. Experimental

2.1. General

All chemicals were purchased from Fluka (Buchs, Switzerland), Sigma (Steinheim, Germany) and Merck (Darmstadt, Germany), unless stated otherwise. NMR spectroscopy experiments were performed on an ARX300 (300.13 MHz for ^{1}H and 75.5 MHz for ^{13}C, Bruker, Karlsruhe, Germany), using the δ scale (ppm) for chemical shifts; ^{13}C-spectra were edited using DEPT techniques. *J* values are given in Hz. Mass spectra were recorded on a QP2010 GC–MS device (electron impact, 70 eV, Shimadzu, Japan). The 3DM database [17] is accessible under http://fungen.wur.nl/ABHDB. *Escherichia coli* NovaBlue singles and BL21 (DE3) cells were obtained from Novagen. PCR primers designed towards the *Nocardia farcinica* esterase were ordered from MWG-Eurofins (Germany). Synthetic genes were obtained from GenScript USA Inc. (New Jersey, USA) and transformed into competent *E. coli* BL21 cells. KOD hot start DNA polymerase was obtained from Novagen. The pET-YSBLIC3C vector was obtained from the Structural Biology Laboratory (University of York). Restriction enzymes were purchased from New England Bio Labs. PCR clean-up and mini-prep kits were purchased from Qiagen, and a gel extraction kit from Sigma Aldrich. Isopropyl β-D-thiogalactopyranoside (IPTG) was purchased from Melford Labs. The homology models of EstA4, EstA5, EstA6 were created using the PHYRE web server (http://www.sbg.bio.ic.ac.uk/~phyre/). The hit was discovered based on the template of the protein with the PDB code c2c7bA.

2.2. Synthesis of tertiary alcohol esters

(*R*,*S*)-2-(Pyridin-2-yl)but-3-yn-2-yl acetate (**1d**), (*R*,*S*)-2-(pyridin-4-yl)but-3-yn-2-yl acetate (**1b**) and (*R*,*S*)-2-(tert-butylcarbamoyl)-1,1,1-trifluorobut-2-yl acetate (**1e**) were prepared as described [13,15]. 2-Hydroxy-2-methyl-1-phenylbutane-1-one (**2f**) was prepared from 2-hydroxy-2-methylbutanoic acid by formation of an intermediate pyrrolidinyl amide and subsequent arylation (818 mg, 62%) [21]. The spectroscopic data matched literature data. Gossonorol (**2g**) was prepared by addition of toluyl-magnesium bromide to 6-methyl-5-heptene-2-one as described [4]. The spectroscopic data matched literature data [4]. Preparation of 2-acetoxy-2-methyl-1-phenylbutane-1-one (**1f**) and gossonoryl acetate (**1g**) was made according to Bäckvall et al. [22].

2.2.1. Acetoxy-2-methyl-1-phenylbutane-1-one (*1f*)

(650 mg, 82% yield). ^{1}H NMR: δ = 0.99 (t, 3H, *J* = 7.5 Hz, CH_3), 1.69 (s, 3H, CH_3), 1.98 (s, 3H, CH_3), 2.00–2.3 (m, 2H, CH_2), 7.4 (m, 3H, H–Ar), 8.03 (d, 2H, H–Ar). ^{13}C NMR: δ = 7.6, 21.2, 21.3, 30.6, 87.0, 128.29, 128.33, 132.33, 134.9, 179.0, 199.1. MS (EI): 177 (M+-43), 159, 145, 132, 115, 105, 73, 43.

2.2.2. Gossonoryl acetate (*1g*)

^{1}H NMR: δ = 1.51 (s, 3H, C(CH_3)2x1), 1.64 (s, 3H, C(CH3)2x1), 1.82 (s, 3H, CCH_3), 1.85–2.02 (4H, m, CH_2CH_2), 2.05 (s, 3H, $COCH_3$), 2.3 (s, 3H, Ar–CH_3), 5.04 (t, 1H, CCH), 7.2 (m, 5H, H–Ar). ^{13}C NMR: δ = 17.49, 20.95, 22.23, 22.51, 24.91, 25.61, 42.22, 83.86, 123.7 124.47, 128.83 131.75 137.27, 141.96, 169.67. MS (EI): 201, 91, 77, 69, 43, 41.

2.3. Cloning of GGG(A)X motif esterases from N. farcinica

From the genomic DNA of *N. farcinica*, the GGG(A)X motif esterases EstA1, EstA2, and EstA3 (accession numbers: Q5YP18, Q5YQP8, Q5YPM0 respectively) were amplified using the following oligonucleotide primers with ligation independent cloning (LIC) specific sites EstA1: 5′-CCAGGGACCAGCAATGGACAACGTGGTCG-AAGCGCCCTCG-3′ and 5′-GAGGAGAAGGCGTTATGCACGGCAAGCT-GTCGAGGGGACT-3′; EstA2: 5′-CCAGGGACCAGCAATGACCATCCG-ATACGACACCACCGTC-3′ and 5′-GAGGAGAAGGCGTTAGCTGGTCC-GCCAGCCGAAGTCGACT-3′; EstA3: 5′-CCAGGGACCAGCAATGGT-GGCAACGATCGACATCACGACC-3′ and 5′-GAGGAGAAGGCGT-TAGCAGTCCCACGGCTGGGACTGGACT-3′ in a standard reaction mixture (0.4 μM of each primer, 0.2 mM dNTPs, 1 unit of KOD hot start DNA polymerase, 1 mM $MgSO_4$, 10× buffer, 50 ng template DNA, 10% (v/v) DMSO, and water to 50 μL) using a temperature cycling program of: 4 min at 94 °C, followed by 35 cycles of: 1 min at 94 °C, 1 min at 55 °C, 1.5 min at 72 °C, with a final extension step for 3 min at 72 °C. The band from agarose gel electrophoresis was excised and the DNA extracted (gel extraction kit – Sigma-Aldrich) before determining the concentration using a spectrophotometer. The purified PCR product was cloned into the cleavable N-terminally his-tagged pET-YSBLIC3C vector using a ligation independent cloning protocol as described previously [23,24]. Transformation of the plasmid into chemocompetent *E. coli* NovaBlue cells, was carried out by incubating on ice for 5 min, followed by a heat-shock at 42 °C for 30 s, and then incubation on ice for a further 5 min before the addition of 0.5 mL of LB medium and incubation at 37 °C for 1 h. Transformed cells were plated onto LB agar plates containing kanamycin (100 μg mL^{-1}) and incubated at 37 °C overnight. Several colonies were picked and the plasmids isolated. Sanger sequencing (Technology Facility, Department of Biology, University of York) of cloned inserts was used to verify that genes contained no mutations.

2.4. Expression and purification of recombinant esterases

500 mL cultures of *E. coli* BL21 (DE3) cells containing the transformed plasmid were grown in LB media containing appropriate antibiotics (EstA1: kanamycin 100 μg mL^{-1}, EstA4 and EstA5 ampicillin 100 μg mL^{-1} and chloramphenicol 50 μg mL^{-1}) at 37 °C until an $OD_{600\,nm}$ 0.5, before inducing with IPTG (0.1 mM) and growing

overnight at 20 °C. Co-expression in the presence of appropriate plasmid encoding for chaperones was performed following the instruction of the Takara kit manual (Takara Bio Inc.). Expression of the chaperone was induced with the appropriate inducer at $OD_{600\,nm}$ 0.3. Cells were harvested by centrifugation (4 °C, 45 min, 6000 × *g*) and the cell pellet was re-suspended in 50 mM Tris/HCl buffer (300 mM NaCl, pH 7.1). The cells were lysed by sonication. The cell debris was removed by centrifugation using a Sorvall RC5B – SS34 centrifuge (4 °C, 20 min, 8000 × *g*) before retaining the soluble cell extract, which was filtered using a 0.45 μm filter (Millipore – PES membrane).

A 5 mL HiTrap chelating nickel column was pre-equilibrated with 25 mL of 0.1 M Ni_2SO_4 followed by 25 mL of the re-suspension buffer (50 mM Tris/HCl buffer, 300 mM NaCl, pH 7.1). The filtered cell extract was loaded, and the unbound protein eluted in a 30 mL wash with 30 mM imidazole (50 mM Tris/HCl buffer, 300 mM NaCl, pH 7.1). A gradient from 30 to 500 mM imidazole was run over a volume of 100 mL. The bound protein of EstA1 eluted over the range of 250–300 mM imidazole. EstA4 and EstA5 eluted between 20 and 100 mM imidazole.

A HiLoad Superdex S200 16/60 gel filtration column was pre-equilibrated with 50 mM Tris/HCl buffer (pH 7.1) containing 300 mM NaCl. 2 mL of concentrated pooled Ni column fractions was loaded and run with the same buffer. 5 mL fractions were collected with the protein eluting at 80 mL. Proteins were also analyzed by a 12% separating and 4% stacking sodium dodecyl sulphate polyacrylamide gel. After electrophoresis the gel was first activity-stained with α-naphthylacetate and Fast Red followed by Coomassie brilliant blue staining. From the gels of purified EstA4 and EstA5, bands were cut out and the amino acid sequence was confirmed by MALDI-Tof sequencing.

2.5. Enzymatic activity in the hydrolysis of pNP esters and amides

Esterase activity was determined spectrophotometrically by hydrolysis of *p*-nitrophenyl esters of different chain length (C2, C4, C6, C8, C10, C14, 1 mM) and *p*-nitrophenyl butyranilide (*p*NPB, 1 mM) in sodium phosphate buffer (10 mM, pH 7.4) and 10% (v/v) DMSO. Released *p*-nitrophenol (*p*NP) and *p*-nitroaniline (*p*NA) were quantified at 410 nm (*p*NP: $\varepsilon = 11.9 \times 10^3\ M^{-1}\ cm^{-1}$, *p*NA; $\varepsilon = 9.1 \times 10^3\ M^{-1}\ cm^{-1}$). One Unit (U) of activity was defined as the amount of enzyme releasing 1 μmol *p*NP per min under assay conditions. For the determination of the pH-profile, activity in the hydrolysis of *p*-nitrophenyl acetate (*p*NPA) was determined using the following buffers at a concentration of 100 mM: pyridine (pH 5–6), sodium phosphate (pH 7–8), and CHES (pH 9–10). Extinction coefficients at the different pH's were calculated for *p*NP. Kinetic data in the hydrolysis of *p*NPA were determined using purified esterase solutions at a range of substrate concentrations. Initial rates for amide or ester hydrolysis were used in Eadie–Hofstee plots to calculate V_{max}, k_{cat}, and K_M values.

2.6. Thermostability of esterases

The purified enzyme was dissolved in sodium phosphate buffer (50 mM, pH 7.4) and incubated at different temperatures (30, 40, 50, and 60 °C). Samples were taken after 0.5, 1, 2, 4, 24 h. The residual esterase activity was determined spectrophotometrically by hydrolysis of *p*NPA esters.

2.7. Esterase-catalysed kinetic resolution

To acetates **1a–i** (12 μmol) dissolved in 100 μL co-solvent, 900 μL esterase solution [with a crude esterase concentration of 1–3 mg mL^{-1} dissolved in phosphate buffer (100 mM, pH 7.5)] was added to form a total volume of 1.5 mL. The reaction mixture was shaken in a thermoshaker (Eppendorf, Germany) at 37 °C for a certain time (0.5 h, 1 h, 4 h, and 24 h), after which a 300 μL sample was taken. The sample was extracted twice with 400 μL dichloromethane. The combined organic layers were dried over Na_2SO_4, filtered and transferred to a GC-vial. Enantioselectivity and conversion were calculated according to Chen et al. [25]. The *E*-value of compounds can be calculated based on ee_S and ee_P [25].

2.8. Gas chromatography analysis

Chiral GC-analyses were performed using Hydrodex-β-3B (Column A), Hydrodex-β-TBDAc (Column B) and Hydrodex-γ-TBDAc (Column C) from Machey-Nagel (Düren, Germany) as columns on a GC-2010 gas chromatograph (Shimadzu, Tokyo, Japan). Chiral analysis of **1a–d** was performed as described [13,15]. Chiral analysis of **2i** was performed by using Column C, running isothermally at 110 °C (retention times: 23.8 min, 24.5 min). Chiral analysis of **2g** was also performed using Column C, running isothermally at 140 °C (retention times: 75.1 min, 77.1 min).

3. Results and discussion

3.1. Identification of target esterases

In preliminary work, the publicly available genome of the actinomycete *N. farcinica* IFM 10152 was screened for the presence of genes encoding enzymes containing the GGG(A)X-motif, characteristic of potential TA esterases [2]. Three genes, encoding enzymes termed EstA1, EstA2 and EstA3 were therefore selected for cloning, expression and assay. Of these, genes encoding EstA1 and Est2 were successfully amplified by PCR and cloned into the pET-YSBLIC3C vector using protocols described previously [23,24]. A search of the α/β hydrolase family in the 3DM database revealed three further enzymes of particular interest due to their similarity in sequence-structure alignments to thermostable esterase A (PEstE) from *P. calidifontis* and the metagenome-derived esterase Est8. The enzymes: EstA4 (from *Methylobacterium populi*), EstA5 (*Pelobacter propionicus* DSM 2379), and EstA6 (*Acidivorax* sp. JS42) each showed approximately 50% sequence homology to Est8, which was known to display moderate enantioselectivity in the esterase catalyzed kinetic resolution of bulky aliphatic tertiary alcohol esters. A homology model for EstA4 that was built using the known structure of PEstE as a basis suggested a large degree of structural conservation with only peripheral differences in the tertiary structure (Fig. 1). Based on the analogue structure of *Candida rugosa* lipase (pdb-entry: 1lpm), the alcohol binding pocket was tentatively assigned. Comparison with PEstE revealed some differences, namely regarding the position N-terminal of the catalytic serine, where PEstE bears an aspartate and EstA4 a glutamate. This residue has been identified as a hot-spot residue for the enantioselectivity of GGG(A)X-esterases [2]. Similar observations for closely comparable overall folds were made for EstA5 and EstA6, and it was anticipated that this structure-guided selection of target esterases would result in enzymes which share the same desirable characteristics of thermostability and enantioselective activity towards bulky tertiary alcohol esters.

3.2. Expression of esterases

Soluble expression of EstA1 was achieved in *E. coli* BL21 cells with overnight incubation at 20 °C. EstA2 and EstA6 could not be expressed in the soluble fraction despite testing growth temperatures, time-periods, cell types, and also different re-suspension buffers. EstA4 and 5 were expressed in low amounts in the soluble fraction. A summary of expression and confirmation of esterase activity is shown in Table 1. Co-expression with chaperones using

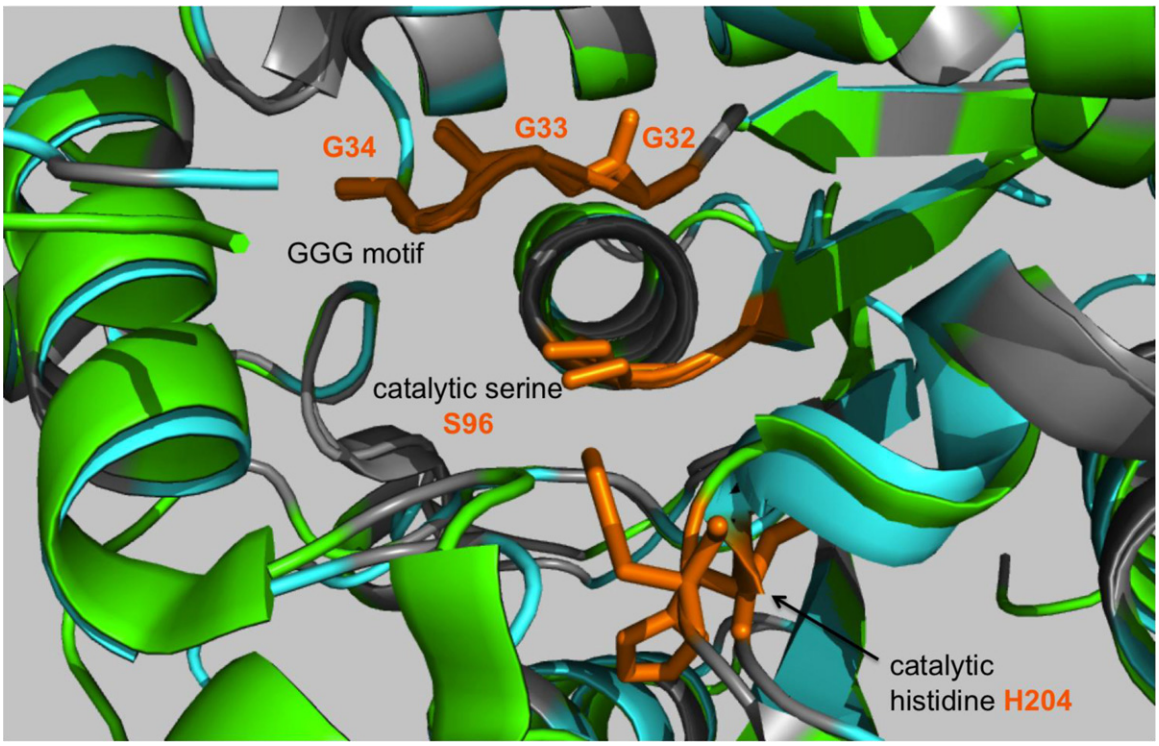

Fig. 1. Comparison between a homology model using the Phyre program (http://www.sbg.bio.ic.ac.uk/~phyre/) created for EstA4 from *Methylobacterium populi* (based on the template of a protein with the PDB code c2c7bA) and the structure of PEstE esterase from *P. calidifontis* (PDB code: 2wir). Regions in the structure which share identical sequence similarity are highlighted in grey, whilst differences belonging to the model of EstA4 are shown in cyan, and those due to PEstE in green. The catalytic serine, catalytic histidine and GGG motifs are also shown in orange together with the corresponding residue numbers as found in the 3DM database. (For interpretation of the references to colour in this figure legend, the reader is referred to the web version of the article.)

a commercially available kit was tested; however no significant improvement in the soluble expression of these esterases could be achieved. Purification of EstA1 was afforded by nickel affinity chromatography followed by gel filtration, whilst EstA4 and EstA5 could be purified to homogeneity solely *via* the use of a nickel column.

3.3. Characterisation of esterase activity

Kinetic parameters in the hydrolysis of *p*NPA were determined using purified esterases. A broad range of activities towards *p*NPA were demonstrated by the three purified esterases, leading to very different kinetic parameters. EstA4 was found to yield the highest turnover of substrate with a k_{cat} of 32.32 s^{-1} (K_M = 2.36 mM), when compared to EstA1 (k_{cat} = 2.73 s^{-1}, K_M = 1.20 mM), and EstA5 (k_{cat} = 0.09 s^{-1}, K_M = 7.23 mM). For determination of the optimum pH for esterase activity, the rate of hydrolysis of *p*NPA was measured between pH 5 and 10 using different buffers at 100 mM concentration. EstA4 and EstA5 both showed pH 8 to be optimal for activity, whilst EstA1 showed highest rate of ester hydrolysis at pH 7.5.

The thermostability of the soluble esterases was measured by determining the percentage of activity remaining towards *p*NPA after pre-incubation of each enzyme at a range of temperatures for defined periods of time prior to analysis (Fig. 2). At lower temperatures of 20 °C and 37 °C EstA1 tended to show more stability than EstA4 and EstA5 with between 75 and 85% of activity remaining after 4 h incubation at these temperatures, when compared to 40–65% for EstA4 and 35–60% for EstA5 over the same time period. Disappointingly, none of the three esterases showed any activity towards *p*NPA when pre-incubated at 60 °C for 30 min. Stability at 50 °C for each of the three esterases was found to be low with 60–75% of activity lost after pre-incubation at this temperature for 30 min. EstA4 showed approximately 20% activity remaining towards *p*NPA after 4 h incubation at 50 °C, during which time no activity could be observed for EstA1 and EstA5. All three esterases showed preference for the hydrolysis of short-chain *p*NP esters (Fig. 3). Hydrolysis of a series of *p*NP esters with increasing chain-length confirmed activity up to C8 for all esterases.

Table 1
Expression of esterases originating from functional-based screening, and structure-guided genome mining approaches, and confirmation of activity towards *p*-nitrophenyl acetate.

Esterase	Source	Accession code	Expression/solubility	Activity towards *p*NPA (Units/mL)
Functional-based screening				
EstA1	*N. farcinica*	Q5YP18	20 °C, o/n[a], soluble	22.13
EstA2	*N. farcinica*	Q5YQP8	Insoluble	–
EstA3	*N. farcinica*	Q5YPM0	Not cloned	–
Structure-guided				
EstA4	*M. populi*	B1ZHM1	20 °C, o/n, soluble	19.20
EstA5	*P. propionicus* DSM 2379	A1AUW3	20 °C, o/n, soluble	0.02
EstA6	*Acidivorax* sp. JS42	A1W6M8	Insoluble	–

[a] Overnight incubation.

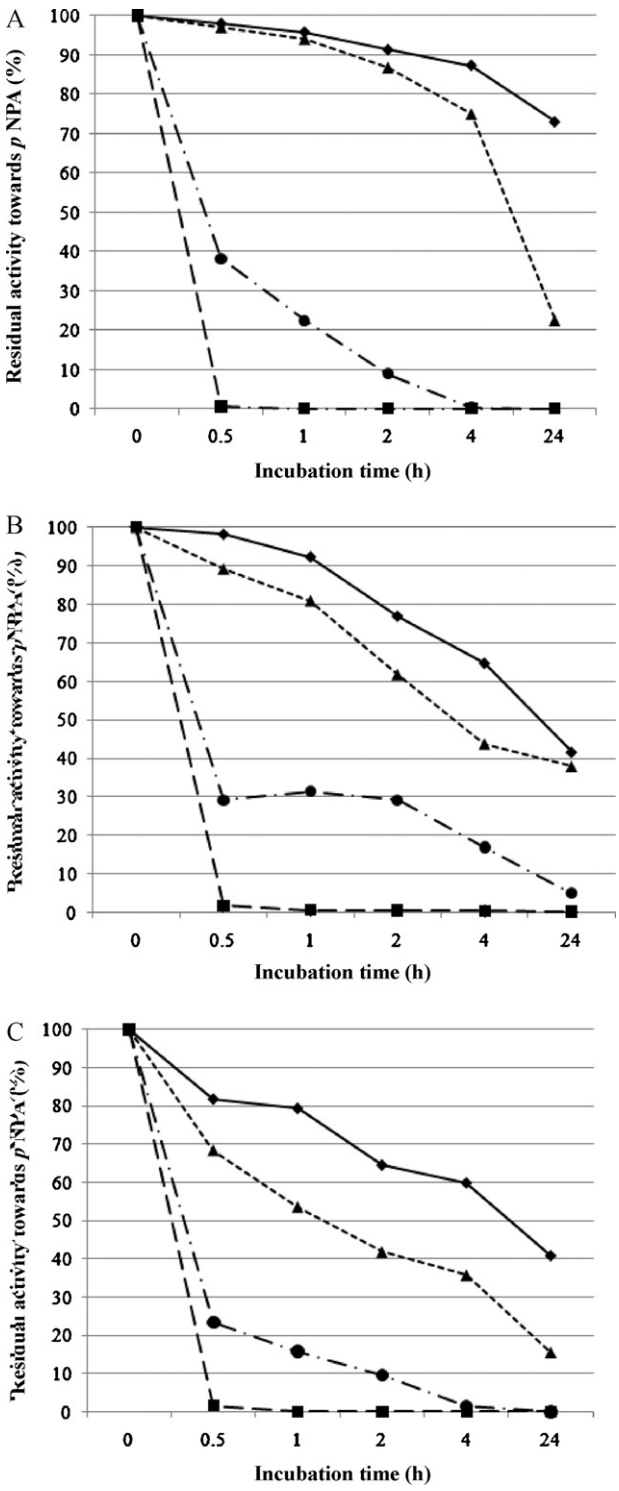

Fig. 2. Measurement of thermostability of purified esterases. The graph shows the residual activity towards *p*NPA after pre-incubation of the enzymes (EstA1 (A), EstA4 (B), and EstA5 (C)) for defined time-periods at the following temperatures: 20 °C (♦), 37 °C (▲), 50 °C (●), and 60 °C (■). Incubation time-points on the *x*-axis are not shown proportionally.

3.4. Kinetic resolutions

EstA1, EstA4 and EstA5 were then assessed for activity towards a range of tertiary alcohol esters **1a–h** and the secondary ester menthyl acetate **1i** (Fig. 4). Substrate diversity encompassed: pyridine-derived tertiary alcohol acetates **1b–d**, bulky aliphatic **1e**

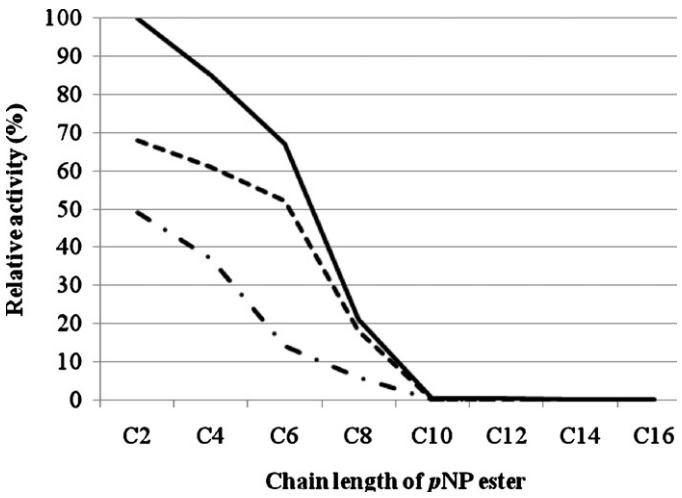

Fig. 3. Specificity of EstA1 (solid line), EstA4 (dotted line), and EstA5 (dashed line) in the hydrolysis of *p*NP esters of differing carbon chain length. Activity was measured relative to the EstA1catalysed hydrolysis of the C2 chain-length ester of *p*NP.

and aromatic **1g** acetates; in addition to tertiary esters bearing fluorinated **1a** and keto- **1f** substituents. These substrates were included in order to examine the extent of structural preference within this class of esters by the isolated enzymes (Tables 2 and 3). Many of these compounds were selected due to their relevance and desirability in fine chemical and pharmaceutical industries. To serve as a comparison for TA esterase activity in the generation of linalool; another monoterpene alcohol of significant interest for the flavour and fragrance industries, menthol, was chosen to investigate enantioselective hydrolysis of a less sterically demanding acetate. Activity towards this secondary alcohol acetate **1i** was found with each of EstA1, EstA4, and EstA5. In the case of EstA1 a high enantioselectivity ($E > 100$) was also observed. EstA4 was active in the hydrolysis of *ortho*-, *meta*- and *para*-pyridine substituted tertiary alcohol esters **1a–c**, although a low enantioselectivity was observed in each case ($E < 5$). Superior enantioselectivity ($E = 10$) in the hydrolysis of **1a** was achieved using EstA1, whilst both this esterase and EstA4 displayed moderate enantioselectivity ($E = 10$ and 24 respectively) in the hydrolysis of the fluorinated tertiary alcohol acetate **1d**. EstA5 was inactive towards each of the sterically challenging TA substrates, and the low k_{cat} and high K_M values for hydrolysis of *p*NPA suggest perhaps why these particular TA acetates are not readily accepted by this enzyme. Encouragingly, EstA1 and EstA5 were both active towards the bulky gossonorol compound **1g**, which shows that both enantiomers of this natural compound are accessible by esterase-catalysed kinetic resolution. However, enantioselectivity was disappointing in both cases ($E < 5$). Unfortunately the activity of EstA1 and EstA4 did not extend to the

Table 2
Enantioselectivity of GGG(A)X esterases towards tertiary alcohol acetates **1a–h**, and the less sterically demanding secondary alcohol ester menthyl acetate **1i**.

Enzyme / Substrate	1a	1b	1c	1d	1e	1f	1g	1h	1i
EstA1									
EstA5									
EstA4									

No conversion; E<5; 5<E<20; 20<E<50; 50<E

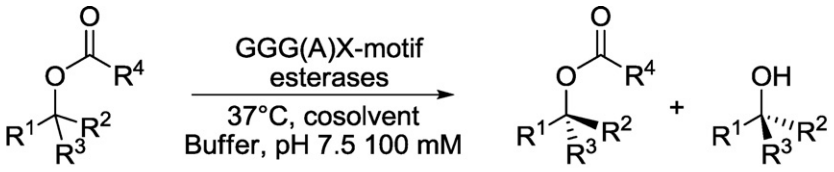

a: R^1 = Ph, R^2 =CF_3 , R^3 = CH≡CH, R^4 = CH_3
b: R^1 = 4'-pyridyl, R^2 = CH_3, R^3 = C≡CH, R^4 = CH_3
c: R^1 = 3'-pyridyl, R^2 = CH_3, R^3 = C≡CH, R^4 = CH_3
d: R^1 = 2'-pyridyl, R^2 = CH_3, R^3 = C≡CH, R^4 = CH_3
e: R^1 = C_2H_5, R^2 = CF_3, R^3 = *N*-(*tert*-butyl)acetamide, R^4 = CH_3
f: R^1 = acetophenyl, R^2 = C_2H_5, R^3 = CH_3, R^4 = CH_3
g: R^1 = 4'-methylphenyl, R^2 = 2-methylhex-2-enyl, R^3 = CH_3
h: **1h** = 3,7-dimethylocta-1,6-dien-3-yl acetate, **2h** = 3,7-dimethylocta-1,6-dien-3-ol
i: **1i** = 2-isopropyl-5-methylcyclohexyl acetate, **2i** = 2-isopropyl-5-methylcyclohexanol

Fig. 4. Enzymatic kinetic resolution of tertiary alcohol acetates **1a–h** and secondary alcohol acetate **1i** to the corresponding alcohols **2a–i**.

Table 3
Kinetic resolution of **1a–i** with GGG(A)X-hydrolases after 1 h reaction time.

Entry	Substrate	Enzyme	%ee_S[a]	%ee_P[a]	c (%)[b]	E[b]
1	1a	EstA1	78	66	52	10
2	1a	EstA5	n.d.[c]	n.d.	n.d.	n.d.
3	1a	EstA4	15	18	45	2
4	1b	EstA1	43	45	49	4
5	1b	EstA5	n.d.	n.d.	0	n.d.
6	1b	EstA4	35	42	47	3
7	1c	EstA1	n.d.	n.d.	0	n.d.
8	1c	EstA5	n.d.	n.d.	0	n.d.
9	1c	EstA4	20	24	55	2
10	1d	EstA1	n.d.	n.d.	0	n.d.
11	1d	EstA5	n.d.	n.d.	0	n.d.
12	1d	EstA4	99	65	60	24
13	1e	EstA1	n.d.	n.d.	0	n.d.
14	1e	EstA5	n.d.	n.d.	0	n.d.
15	1e	EstA4	n.d.	n.d.	0	n.d.
16	1f	EstA1	n.d.	n.d.	0	n.d.
17	1f	EstA5	n.d.	n.d.	0	n.d.
18	1f	EstA4	n.d.	n.d.	0	n.d.
19	1g	EstA1	n.d.	6	43	1
20	1g	EstA5	n.d.	n.d.	0	n.d.
21	1g	EstA4	n.d.	10	48	1
22	1h	EstA1	n.d.	n.d.	0	n.d.
23	1h	EstA4	n.d.	n.d.	0	n.d.
24	1h	EstA5	n.d.	n.d.	0	n.d.
25	1i	EstA1	n.d.	99	23	>100
26	1i	EstA5	n.d.	68	41	8
27	1i	EstA4	n.d.	61	32	5

[a] As determined by chiral GC-analysis.
[b] Calculated from ee_S and ee_P.
[c] n.d., not determined.

bulky aliphatic compound **1e** or the keto-substituted TA acetate **1f**. Linalyl acetate **1 h** was found not to be converted by any of the three esterases, although as previously reported in the literature [17,18] this is not uncommon for esterases.

4. Conclusions

Potentially useful esterases for the hydrolysis of sterically hindered tertiary alcohol acetates were identified *via* genome sequence analysis, and by using structural information from the α/β-Hydrolase Fold Enzyme Family covered in the 3DM Database. All esterases identified were found to contain the GGG(A)X motif within their peptide sequence, which is known to confer hydrolase activity towards these demanding substrates. Esterase activity was characterised for three enzymes, two of which EstA1 and EstA4 proved to be active and enantioselective (*E*-values up to 24) towards the kinetic resolution of TAs with diversity encompassing *ortho*-, *meta*- and *para*-pyridine substituted tertiary alcohol esters **1b–d**, the fluorinated derivatives **1a** and **1e**, and gossonorol **1g**, which harbours bulky aliphatic and aromatic groups. Each of the soluble esterases also displayed activity towards the less sterically challenging secondary alcohol ester menthyl acetate. Interestingly, EstA1 from *N. farcinica* displayed excellent enantioselectivity

($E > 100$) in the preparation of 1(*R*)-menthol **2i**; and which alongside EstA4 from *M. populi*, shows that esterases identified through genome mining are potential biocatalysts for the kinetic resolution of secondary and tertiary alcohols. Despite the moderate enantioselectivity displayed towards tertiary alcohols by these esterases; this investigation provides a basis for further protein engineering studies to improve enantioselectivity towards these sterically demanding substrates.

Acknowledgements

European Social Funds and the VentureCup M-V (UG09005) are gratefully acknowledged for financial support. G.S.N. is grateful to the DAAD (Grant: A/07/95194) and the Vietnamese ministry of Education and Training (Grant: 3413/QDBGDDT-VP). M.L.T. also acknowledges the Biotechnology and Biological Sciences Research Council and Botanix Ltd. for their financial support. We thank Fabian Steffen-Munsberg for support in the optimization of expression conditions and Anita Gollin (both University of Greifswald) for synthesis of tertiary alcohol acetates.

References

[1] P. Cozzi, R. Hilgraf, N. Zimmermann, Eur. J. Org. Chem. (2007) 5969–5994.
[2] R. Kourist, P. de Maria, U. Bornscheuer, ChemBioChem 9 (2008) 491–498.
[3] T. Kishimoto, A. Wanikawa, N. Kagami, K. Kawatsura, J. Agric. Food Chem. 53 (2005) 4701–4707.
[4] K. Abecassis, S.E. Gibson, Eur. J. Org. Chem. 2010 (2010) 2938–2944.
[5] R. Gregory, Chem. Rev. 99 (1999) 3649–3682.
[6] G. Yao, S. Haque, L. Sha, G. Kumaravel, J. Wang, T. Engber, E. Whalley, P. Conlon, H. Chang, W. Kiesman, R. Petter, Bioorg. Med. Chem. Lett. 15 (2005) 511–515.
[7] J. Ekegren, T. Unge, M. Safa, H. Wallberg, B. Samuelsson, A. Hallberg, J. Med. Chem. 48 (2005) 8098–8102.
[8] F. Russo, F. Wångsell, J. Sävmarker, M. Jacobsson, M. Larhed, Tetrahedron 65 (2009) 10047–10059.
[9] I. Osprian, A. Steinreiber, M. Mischitz, K. Faber, Biotechnol. Lett. (1996).
[10] M. Pogorevc, K. Faber, J. Mol. Catal. B: Enzym. 10 (2000) 357–376.
[11] M. Pogorevc, U. Strauss, M. Hayn, K. Faber, Monatsh. Chem. 131 (2000) 639–644.
[12] A. Schlacher, T. Stanzer, I. Osprian, M. Mischitz, E. Klingsbichel, K. Faber, H. Schwab, J. Biotechnol. 62 (1998) 47–54.
[13] G. Nguyen, R. Kourist, M. Paravidino, A. Hummel, J. Rehdorf, R. Orru, U. Hanefeld, U. Bornscheuer, Eur. J. Org. Chem. (2010) 2753–2758.
[14] N. Kato, S. Shibayama, K. Munakata, C. Katayama, J. Chem. Soc. D (1971) 1632–1633.
[15] R. Kourist, G. Nguyen, D. Strübing, D. Böttcher, K. Liebeton, C. Naumer, J. Eck, U. Bornscheuer, Tetrahedron: Asymmetry 19 (2008) 1839–1843.
[16] E. Henke, E. Pleiss, U. Bornscheuer, Angew. Chem. Int. Ed. 41 (2002) 3211–3213.
[17] R. Kourist, H. Jochens, S. Bartsch, R. Kuipers, S.K. Padhi, M. Gall, D. Böttcher, H.-J. Joosten, U.T. Bornscheuer, ChemBioChem 11 (2010) 1635–1643.
[18] A. Bassegoda, G. Nguyen, M. Schmidt, R. Kourist, P. Diaz, U.T. Bornscheuer, ChemCatChem 2 (2010) 962–967.
[19] H. Jochens, D. Aerts, U.T. Bornscheuer, Protein Eng. Des. Sel (2010), doi:10.1093/protein/gzq1071.
[20] H. Jochens, U.T. Bornscheuer, ChemBioChem 11 (2010) 1861–1866.
[21] L. Tan, C. Chen, W. Chen, L. Frey, A. King, R. Tillyer, F. Xu, D. Zhao, E. Grabowski, P. Reider, P. O'Shea, P. Dagneau, X. Wang, Tetrahedron 58 (2002) 7403–7410.
[22] J. Bäckvall, R. Nordberg, J. Nystroem, J. Org. Chem. 46 (1981) 3479–3483.
[23] C. Aslanidis, P.J. Dejong, Nucleic Acids Res. 18 (1990) 6069–6074.
[24] D. Bonsor, S.F. Butz, J. Solomons, S. Grant, I.J.S. Fairlamb, M.J. Fogg, G. Grogan, Org. Biomol. Chem. 4 (2006) 1252–1260.
[25] C. Chen, Y. Fujimoto, G. Girdaukas, C. Sih, J. Am. Chem. Soc. 104 (1982) 7294–7299.